Critical electric field for transition of thermionic field emission/field emission transport in heavily doped SiC Schottky barrier diodes

View Online   Export Citation   CrossMark

Masahiro Hara,[1,a)] (iD) Hajime Tanaka,[1,2] (iD) Mitsuaki Kaneko,[1] (iD) and Tsunenobu Kimoto[1] (iD)

AFFILIATIONS

[1]Department of Electronic Science and Engineering, Kyoto University, Nishikyo, Kyoto 615-8510, Japan
[2]Division of Electrical, Electronic and Infocommunications Engineering, Osaka University, Suita, Osaka 565-0871, Japan

[a)]Author to whom correspondence should be addressed: hara@semicon.kuee.kyoto-u.ac.jp

ABSTRACT

In this study, n-type SiC Schottky barrier diodes (SBDs) with various doping concentrations ($N_d = 4 \times 10^{15}$–$1 \times 10^{19} \mathrm{cm}^{-3}$) were fabricated, and their forward and reverse current–voltage (I–V) characteristics were analyzed focusing on tunneling current. Numerical calculation with the fundamental formula of tunneling current gives good agreement with experimental forward and reverse I–V curves in the heavily doped SiC SBDs ($N_d > 2 \times 10^{17} \mathrm{cm}^{-3}$). The analysis of the energy where electron tunneling most frequently occurs revealed that field emission (FE) tunneling dominates conduction instead of thermionic field emission (TFE) under a higher electric field in reverse-biased heavily doped SiC SBDs, while forward I–V characteristics are described only by TFE. In addition, the critical electric field for the TFE–FE transition is quantitatively clarified by carefully considering the sharply changing electric field distribution in SiC with a high donor concentration.

Published under an exclusive license by AIP Publishing. https://doi.org/10.1063/5.0088681

4H-Silicon carbide (SiC) has unique material properties such as wide bandgap (3.26 eV) and high critical electric field (∼3 MV/cm) which make it possible to significantly improve efficiency in power semiconductor devices.[1–3] Thanks to the intensive studies on material properties and device processing over the years, SiC Schottky barrier diodes (SBDs) and metal-oxide-semiconductor field-effect transistors (MOSFETs) have already been in mass production, achieving considerable loss reduction in power converters and inverters.[4,5] On the other hand, there remain several technical issues that hinder further improvement in the performance and reliability of SiC devices. Achieving sufficiently low contact resistivity of Ohmic contacts ($<10^{-6} \Omega \, \mathrm{cm}^2$) with a low thermal budget is highly demanded among those critical issues.[6–8]

Since the wide bandgap of SiC makes it difficult to form a metal/SiC interface with a low barrier just by depositing an electrode metal, post-metallization annealing at a very high temperature (∼1000 °C) is generally performed to obtain low contact resistivity. Until now, an interfacial layer formed during the high-temperature annealing has been studied in detail from the standpoint of structural analysis.[9–12] Despite continuous research, however, the correlation between such interfacial reactions and electrical characteristics is not quantitatively understood even now. Consequently, the mechanism for obtaining

Ohmic behavior with the high-temperature annealing is still unclear, and thus, there are no guidelines to design and form good Ohmic contacts on SiC. Interfacial reactions during the high-temperature treatment are so complicated that it is very tough to reveal the conduction mechanism on such annealed contacts. For instance, an alloyed interfacial layer should be much different from the original SiC, like having very different physical properties and/or containing many kinds of defects. Although tunneling of carriers is generally considered to be responsible for Ohmic conduction, these factors should affect the conduction mechanism and the Ohmic behavior on SiC contacts can no longer be described by the pure tunneling process. Therefore, understanding the carrier transport at a metal/SiC junction without the high-temperature annealing should come first and then the relevant changes caused by the annealing should be systematically investigated.

Since one can obtain a Schottky contact in the case of just depositing a metal on SiC, carrier transport in SiC SBDs is focused on. Ohmic contacts are generally formed on SiC with a high doping concentration, and thus, carrier transport in SBDs fabricated with heavily doped SiC has been investigated.[13,14] It should be supplemented that technological importance of Schottky contacts on heavily doped SiC has recently been recognized and an advantage in introducing a heavily doped SiC layer to power SBDs has been discussed.[14,15]

The authors previously reported that a high electric field ($>2\,MV/cm$) even under a forward bias in heavily doped SiC SBDs ($>10^{17}\,cm^{-3}$) leads to thermionic field emission (TFE) current which is explained by a tunneling process of thermally excited carriers.[13,16] Note that TFE current is commonly observed as the reverse leakage in high-voltage SBDs fabricated with lightly doped wide-bandgap semiconductor materials.[17–20] Considering the case when a reverse bias is applied in heavily doped SiC SBDs, on the other hand, the electric field should become much higher, and tunneling current based on field emission (FE) which describes a tunneling process without thermal excitation of carriers likely appears.[21] The analytical conditions for the TFE and FE models have been discussed in detail from the viewpoint of their dependences on temperature[21,22] and electric field,[18,21] which are important factors in the tunneling process. With regard to the electric field dependence of the tunneling process, these previous works have dealt with a uniformly distributed electric field in a depletion region. Although this assumption is valid for Schottky contacts formed with lightly doped semiconductors, the electric field should change rapidly in the case of high doping concentration, and thus, the conventional analytical conditions are not expected to be applicable to metal/heavily doped semiconductor contacts. Since the contact resistivity predicted from the TFE and FE models is very different from each other, identifying the critical electric field for the TFE–FE transition at metal/heavily doped SiC interfaces is essential for designing Ohmic contacts. However, there have been no reports that systematically investigate the electric field dependence of the tunneling process in heavily doped SiC SBDs.

In this study, Ni/n-type SiC SBDs with various donor concentrations were fabricated, and their forward and reverse current–voltage (I–V) characteristics were analyzed focusing on tunneling current. Since the conditions of the doping concentration and applied voltage were systematically changed, the electric field range dealt with in this experiment is very wide. Therefore, the authors did not use the analytical formula of the TFE or FE model which is derived assuming only one type of tunneling process[18,22] and analyzed I–V characteristics with the fundamental formula of tunneling current.[23] Based on the calculation, the dominant carrier transport mechanism in the heavily doped SiC SBDs was classified as TFE under a forward bias, while both TFE and FE under a reverse bias. In addition, the critical condition of the electric field where dominant tunneling process changes from TFE to FE in the heavily doped SiC SBDs is quantitatively discussed.

In this study, n-type 4H-SiC(0001) substrates with n-type epitaxial layers having various donor concentrations ($N_d = 4.2 \times 10^{15}$, 9.0×10^{15}, 2.0×10^{17}, 2.6×10^{18}, $1.2 \times 10^{19}\,cm^{-3}$) were fabricated. The N_d values were determined by capacitance–voltage (C–V) measurements. The circular-shaped Schottky electrodes with a diameter of 300–600 μm were formed on the epitaxial layers by depositing Ni via resistive heating evaporation. Afterwards, the electrodes were annealed at low temperature ($300\,^\circ$C) to improve the barrier uniformity.[24] The forward and reverse I–V characteristics of the fabricated SBDs were measured at room temperature, and they were analyzed focusing on tunneling current. Although any edge termination structure was not employed in the SBDs, size dependence of the current density was not observed, reflecting very small electric field crowding and negligibly small unideal leakage current at the edge of contacts.

The formula for the calculation of tunneling current used in this study is[23]

$$J_{tunnel} = \frac{A^* T}{k_B} \int P(E) \ln\left[\frac{\exp\{-(E - E_{Fs})/k_B T\} + 1}{\exp\{-(E - E_{Fm})/k_B T\} + 1}\right] dE, \quad (1)$$

where A^* is the effective Richardson constant ($146\,A/cm^2K^2$),[25] T is the absolute temperature, k_B is the Boltzmann constant, E_{Fs} is the Fermi level in the semiconductor, E_{Fm} is the Fermi level in the metal, and E is the energy of an electron along the tunneling direction, respectively. Note that Eq. (1) expresses tunneling from SiC to metal, and tunneling in the opposite direction can be described just by flipping E_{Fs} and E_{Fm}. $P(E)$ is the probability of tunneling and the Wentzel–Kramers–Brillouin (WKB) approximation derives[26]

$$P(E) = \exp\left[-\frac{2\sqrt{2m^*}}{\hbar} \int_{x_{in}}^{x_{out}} \sqrt{V(x) - E}\,dx\right], \quad (2)$$

where m^* is the tunneling effective mass, $\hbar$ is the Dirac constant, x_{in} is the position of an incident carrier, and x_{out} is the position of a transmitted carrier, respectively. The typical values of x_{in} and x_{out} are about 0.01–0.1 nm and 1–10 nm, respectively, while these values depend on the energy of an electron, doping concentration, and applied voltage. As depicted in Fig. 1(a), considering the image force effect,[13,21,27] the energy potential in depletion region in semiconductor, $V(x)$, was assumed to be

$$V(x) = \frac{e^2 N_d}{2\varepsilon_s} x^2 - \frac{e^2 N_d w}{\varepsilon_s} x - \frac{e^2}{16\pi\varepsilon_s x}, \quad (3)$$

where e is the elementary charge, ε_s is the dielectric constant of SiC ($10.32\varepsilon_0$),[24] and w is the depletion layer width. While Eq. (1) does not assume only one type of conduction mechanism of TFE or FE, the dominant conduction mechanism is able to be classified by investigating the energy where tunneling of carriers most frequently occurs (E_{peak}), that gives a peak value in the integrand of Eq. (1), $J(E)$. As mentioned above, TFE or FE is the tunneling process with or without thermal excitation of carriers, respectively. Thus, TFE and FE can be distinguished by whether E_{peak} is higher than or similar to the conduction band edge (E_C) in SiC (forward bias) or E_{Fm} (reverse bias), as shown in Fig. 1(b). In this study, for the heavily doped SiC SBDs ($N_d \geq 2.0 \times 10^{17}\,cm^{-3}$), the tunneling current was calculated with Eq. (1) using the barrier height under the flatband condition [ϕ_{B0}, indicated in Fig. 1(a)] and m^* as parameters, and the dominant carrier transport mechanism was identified based on the above concept. Note that ϕ_{B0} is included in the calculation as $E_{Fm} = -\phi_{B0}$ and $E_{Fs} = -\phi_{B0} + eV$ as depicted in Fig. 1(a), and the built-in potential (V_d) contained in $w = \sqrt{2\varepsilon_s(V_d - V)/eN_d}$ is also related to ϕ_{B0} based on the relationship[28]

$$\phi_{B0} = eV_d + E_C - E_{Fs} + k_B T. \quad (4)$$

Figure 2 shows the experimental and calculated I–V curves of the heavily doped SiC SBDs ($N_d = 1.2 \times 10^{19}$, 2.6×10^{18}, and $2.0 \times 10^{17}\,cm^{-3}$) under (a) forward and (b) reverse biases. Note that the series resistance was extracted from the experimental I–V curves, and the voltage drop by the series resistance was taken into account in plotting the calculated I–V curves. Forward I–V characteristics of the lightly doped SiC SBDs ($N_d = 9.0 \times 10^{15}\,cm^{-3}$) obtained via experiment and calculation based on the well-known thermionic emission
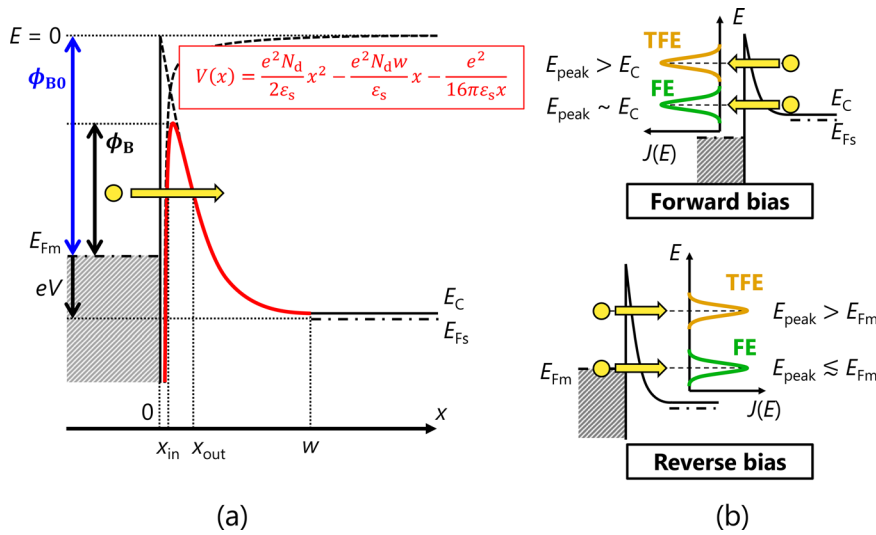
FIG. 1. (a) Band diagram near the metal/SiC Schottky interface assumed for the calculation of tunneling current. (b) Classification between thermionic field emission (TFE) and field emission (FE) under forward and reverse biases.

(TE) model[28] are also shown in Fig. 2(c). The SBDs with $N_d = 4.2 \times 10^{15}\,\mathrm{cm}^{-3}$ showed I–V curves similar to those for $N_d = 9.0 \times 10^{15}\,\mathrm{cm}^{-3}$, to which the TE-based analysis was adaptable (not shown). The reverse current in the lightly doped SiC SBDs (N_d

$\leq 9.0 \times 10^{15}\,\mathrm{cm}^{-3}$) was confirmed to be lower than the detection limit in the measured voltage range (-50 to 0 V). As seen in Figs. 2(a) and 2(b), the tunneling current calculated with Eq. (1) gives good agreement with the experimental curves for both of the forward and reverse
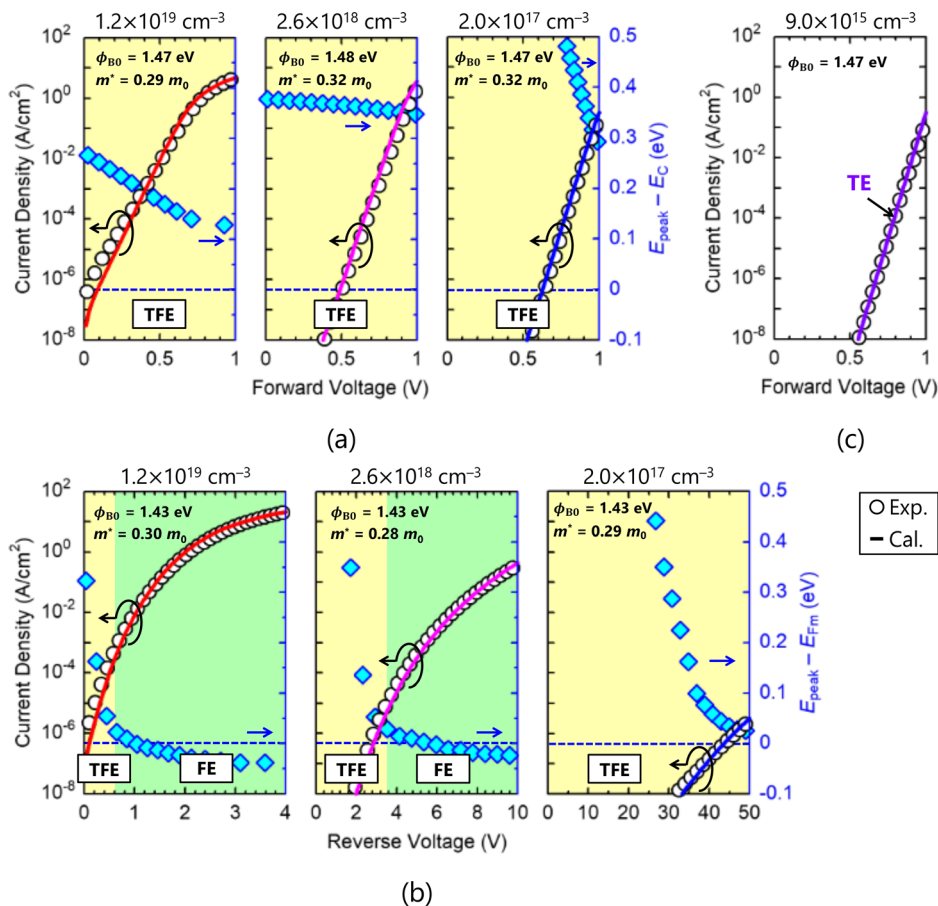

FIG. 2. (a) Forward and (b) reverse I–V characteristics of the Ni/heavily doped SiC SBDs ($N_d = 1.2 \times 10^{19}$, 2.6×10^{18}, and $2.0 \times 10^{17}\,\mathrm{cm}^{-3}$) obtained from experiment and calculation with the fundamental formula of tunneling current. Blue symbols indicate the energy where electron tunneling most frequently occurs (E_{peak}). (c) Forward I–V characteristics of the Ni/lightly doped SiC SBDs ($N_d = 9.0 \times 10^{15}\,\mathrm{cm}^{-3}$) from experiment and TE-based calculation.

I–V characteristics. The small discrepancy in the low voltage region for $N_d = 1.2 \times 10^{19}$ cm^{-3} may be caused by nonideal leakage current resulting from interface states and/or barrier inhomogeneity, etc. Focusing on the reverse characteristics ($N_d = 1.2 \times 10^{19}$ and 2.6×10^{18} cm^{-3}), the authors confirmed that the analytical formula of TFE or FE only[18,22] could not reproduce the experimental curves for the entire voltage range, indicating the necessity for the numerical calculation in the analysis of reverse tunneling current in heavily doped SiC SBDs ($>10^{18}$ cm^{-3}). This is because the carrier transport mechanism changes depending on the applied voltage, as in detail discussed later.

Figure 3 depicts the donor concentration dependence of the barrier height (ϕ_B, including the image force lowering) at zero bias obtained through I–V and C–V measurements in the fabricated SiC SBDs. In the calculation of tunneling current, the amount of the barrier drop by image force ($\Delta\phi$) was obtained by calculating the maximum of $V(x)$, and then ϕ_B was determined by $\phi_{B0} - \Delta\phi$. As for C–V measurements, ϕ_{B0} and $\Delta\phi$ were calculated using V_d and N_d based on Eq. (4) and $\Delta\phi = (e^3 N_d V_d / 8\pi^2 \varepsilon_s^3)^{1/4}$, respectively.[28] As shown in Fig. 3, the barrier heights extracted by the different methods are consistent with each other, and ϕ_{B0} was determined to be 1.43–1.48 eV. It was confirmed that, as the authors reported previously,[13,16] the barrier height under the flatband condition (ϕ_{B0}) is almost independent of N_d, and the decrease in ϕ_B in the heavily doped SiC SBDs is quantitatively explained by strong image force lowering. As for the effective mass, the value of $(0.30 \pm 0.02)m_0$ was obtained from the analysis of tunneling current. This value is nearly equal to the effective mass of $0.33m_0$ at E_C along the c-axis[29] which is the conducting direction in the fabricated SBDs.

The dominant carrier transport mechanism in the heavily doped SiC SBDs under both forward and reverse biases is discussed. The energy difference between E_{peak} and E_C (forward bias) or E_{Fm} (reverse bias) is indicated by blue symbols in Fig. 2. As for the forward I–V characteristics, E_{peak} is higher than E_C in the measured voltage range,

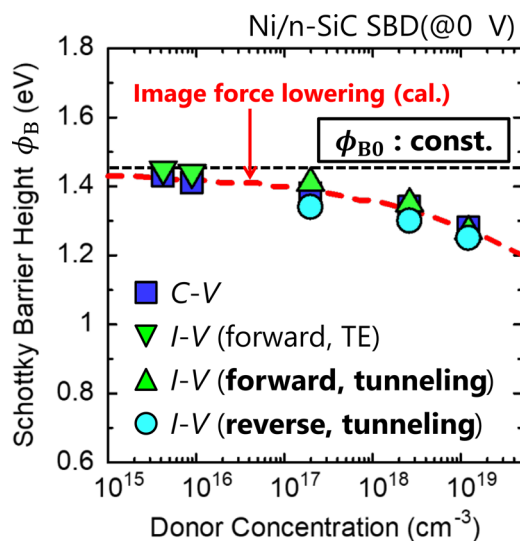indicating that TFE transport is dominant in forward-biased heavily doped SiC SBDs. This result is consistent with our previous study[13] in which the analytical formula of the TFE model[22] was used to calculate the tunneling current. On the other hand, for the reverse I–V characteristics, E_{peak} becomes nearly equal to or lower than E_{Fm} as the applied reverse voltage increases. This result means that the dominant tunneling process changes from TFE to FE due to the higher electric field under the larger reverse bias. By investigating the electric field at the Schottky interface (F_{max}) where the TFE–FE transition is observed, F_{max} of 2.9 MV/cm for $N_d = 1.2 \times 10^{19}$ cm^{-3} and 2.1 MV/cm for $N_d = 2.6 \times 10^{18}$ cm^{-3} were obtained. Here, the boundary between TFE and FE was defined at the energy of $E_{Fm} + 26$ meV, considering the thermal energy of electrons. It is generally understood that the dominant tunneling process is almost uniquely determined by the electric field under a given barrier height.[30] In this context, F_{max} has conventionally been used to discuss the carrier transport in high-voltage SBDs fabricated with lightly doped wide-bandgap semiconductors.[18,31] When using F_{max}, however, the critical electric field where the conduction mechanism changes from TFE to FE is dependent on N_d. Therefore, the authors focused on the fact that the electric field distribution and thereby the potential barrier shape are different among SBDs with different donor concentrations.

Figure 4 depicts the band diagram and the electric field distribution in the depletion region of the heavily doped SiC SBDs ($N_d = 1.2 \times 10^{19}$ and 2.6×10^{18} cm^{-3}) under the bias at the boundary of TFE and FE. Due to the large N_d, the electric field rapidly decreases as
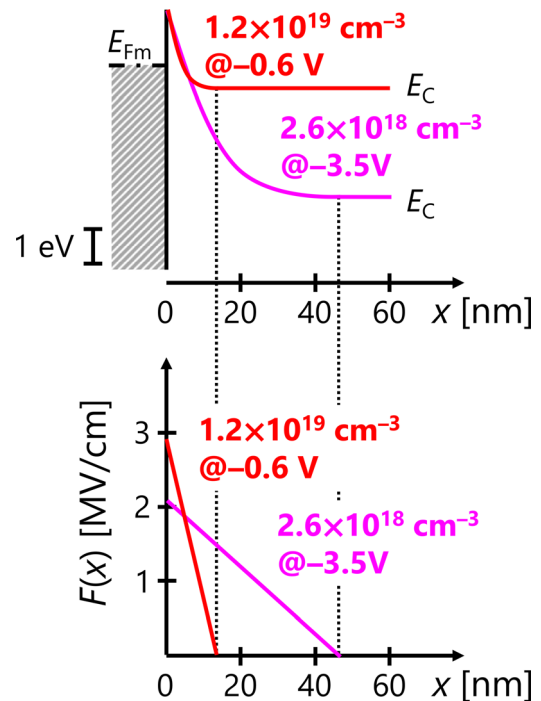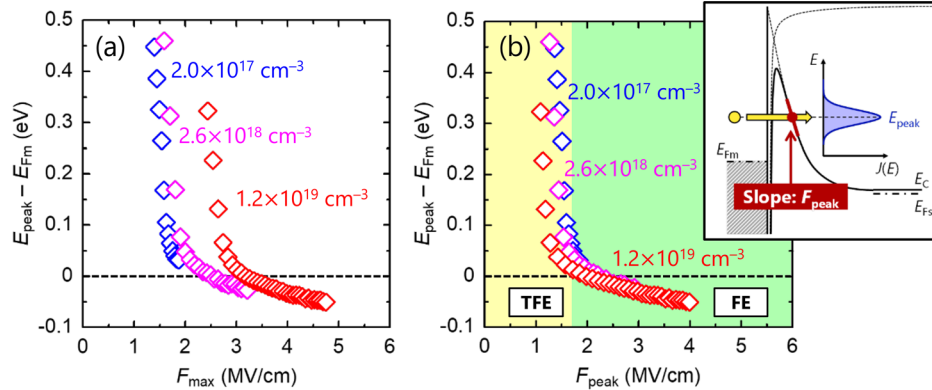

FIG. 4. Band diagram and electric field distribution in the depletion layer near the metal/heavily doped SiC interfaces ($N_d = 1.2 \times 10^{19}$ and 2.6×10^{18} cm^{-3}) under the reverse bias at the boundary of TFE and FE. In the case of the higher doping concentration (1.2×10^{19} cm^{-3}), the electric field sharply decreases as the position becomes far from the interface.

FIG. 3. Donor concentration dependence of barrier height at zero bias obtained from I–V and C–V characteristics.

FIG. 5. E_{peak} vs (a) the electric field at the Schottky interface (F_{max}) and (b) the electric field at the energy of E_{peak} (F_{peak}). Electric field dependence of tunneling process (TFE/FE) is uniquely determined by using F_{peak}.

the position becomes far from the interface in the case of $N_d = 1.2 \times 10^{19} \text{cm}^{-3}$, as shown in Fig. 4. As a result, under the condition where the TFE–FE transition occurs ($E_{peak} \sim E_{Fm}$), the electric field at the energy of E_{peak} (F_{peak}) is calculated to be 1.6 MV/cm, which is much different from F_{max} of 2.9 MV/cm. Therefore, the authors tried to investigate the electric field dependence of tunneling process using F_{peak}. Figure 5 shows the correlation between $E_{peak} - E_{Fm}$ and (a) F_{max} or (b) F_{peak} in the reverse-biased heavily doped SiC SBDs ($N_d \geq 2.0 \times 10^{17} \text{cm}^{-3}$). While the donor-concentration-dependent TFE–FE transition is observed when using F_{max} as shown in Fig. 5(a), F_{peak} at the TFE–FE transition is nearly independent of the donor concentration as seen in Fig. 5(b). Consequently, it turned out that F_{peak} should be used instead of F_{max} to discuss the electric field dependence of the tunneling process of TFE and FE in SBDs especially in the case of high doping concentration. Based on the detailed discussion above, it is concluded that, in the case of metal/heavily doped SiC Schottky interfaces with the barrier height of about 1.4–1.5 eV, the dominant conduction mechanism changes from TFE to FE when the electric field at the energy of E_{Fm} exceeds 1.6–1.7 MV/cm irrespective of the donor concentration.

This concept of using F_{peak} to discuss the change of tunneling process is adoptable when using other kinds of Schottky metal with a different work function. From the viewpoint of Ohmic contact formation, the critical electric field for the TFE–FE transition at low Schottky barriers using a metal with lower work function is especially important. Thus, F_{peak} at the TFE–FE transition was calculated assuming ϕ_{B0} of 0.4 eV, that is the barrier height recently reported for Mg/SiC contacts,[32] and then F_{peak} of 0.8 MV/cm was obtained. This result indicates that the TFE–FE transition occurs under a lower electric field for Schottky contacts with a lower barrier. To fully understand the electric field dependence of the tunneling process and make it useful for designing Ohmic contacts, experimental investigation on the barrier height dependence of the TFE–FE transition is vital. In addition, regarding the fact that the tunneling process changes strongly depending also on the temperature,[21,22] it is indispensable to characterize the temperature dependence of I–V relationship and investigate how a change in the temperature affects the critical electric field for the TFE–FE transition, which is also our future work.

In summary, the authors analyzed the forward and reverse I–V characteristics in heavily doped SiC SBDs and investigated the dominant conduction mechanism in detail. The forward and reverse I–V characteristics of the heavily doped SiC SBDs ($N_d > 2.0 \times 10^{17} \text{cm}^{-3}$) are well reproduced by the tunneling current calculated with the fundamental formula of tunneling current that does not assume only one type of conduction process of TFE or FE. Investigation of the energy where the electron tunneling most frequently occurs (E_{peak}) revealed that TFE transport is dominant under a forward bias in the heavily doped SiC SBDs ($N_d > 2.0 \times 10^{17} \text{cm}^{-3}$), while the higher electric field makes the dominant tunneling process change from TFE to FE in the case of the reverse-biased heavily doped SiC SBDs. Focusing on the electric field at the energy of E_{peak} (F_{peak}), the electric field dependence of the conduction mechanism is uniquely obtained independent of N_d, and the critical condition of the electric field at the boundary of TFE and FE is quantitatively determined. These findings on basic properties at a metal/heavily doped SiC interface should be an essential starting point for a deeper understanding of the carrier transport at Ohmic contacts on SiC. In addition, the proposed concept to analyze the critical electric field for the TFE–FE transition helps design Ohmic contacts on SiC as well as other wide-bandgap semiconductor materials.

AUTHOR DECLARATIONS
Conflict of Interest

The authors have no conflicts to disclose.

DATA AVAILABILITY

The data that support the findings of this study are available within the article.

REFERENCES

[1]A. Itoh, T. Kimoto, and H. Matsunami, IEEE Electron Device Lett. **16**, 280 (1995).
[2]J. A. Cooper, Jr. and A. Agarwal, Proc. IEEE **90**, 956 (2002).
[3]T. Kimoto, Jpn. J. Appl. Phys. **54**, 040103 (2015).
[4]K. Hamada, S. Hino, N. Miura, H. Watanabe, S. Nakata, E. Suekawa, Y. Ebiike, M. Imaizumi, I. Umezaki, and S. Yamakawa, Jpn. J. Appl. Phys. **54**, 04DP07 (2015).

[5]X. She, A. Q. Huang, Ó. Lucía, and B. Ozpineci, IEEE Trans. Ind. Electron. **64**, 8193 (2017).

[6]J. Crofton, L. M. Porter, and J. R. Williams, Phys. Status Solidi B **202**, 581 (1997).

[7]S. Tanimoto, H. Okushi, and K. Arai, in *Silicon Carbide: Recent Major Advances*, edited by W. J. Choyke, H. Matsunami, and G. Pensl (Springer, Berlin/Heidelberg, 2004), pp. 651–669.

[8]F. Roccaforte, P. Fiorenza, G. Greco, R. Lo Nigro, F. Giannazzo, F. Iucolano, and M. Saggio, Microelectron. Eng. **187–188**, 66 (2018).

[9]J. Crofton, P. G. McMullin, J. R. Williams, and M. J. Bozack, J. Appl. Phys. **77**, 1317 (1995).

[10]F. La Via, F. Roccaforte, A. Makhtari, V. Raineri, P. Musumeci, and L. Calcagno, Microelectron. Eng. **60**, 269 (2002).

[11]I. P. Nikitina, K. V. Vassilevski, N. G. Wright, A. B. Horsfall, A. G. O'Neill, and C. M. Johnson, J. Appl. Phys. **97**, 083709 (2005).

[12]S. Tsukimoto, K. Ito, Z. Wang, M. Saito, Y. Ikuhara, and M. Murakami, Mater. Trans. **50**, 1071 (2009).

[13]M. Hara, S. Asada, T. Maeda, and T. Kimoto, Appl. Phys. Express **13**, 041001 (2020).

[14]M. Vivona, G. Greco, M. Spera, P. Fiorenza, F. Giannazzo, A. L. Magna, and F. Roccaforte, J. Phys. D: Appl. Phys. **54**, 445107 (2021).

[15]M. Vivona, F. Giannazzo, and F. Roccaforte, Materials **15**, 298 (2021).

[16]M. Hara, M. Kaneko, and T. Kimoto, Jpn. J. Appl. Phys. **60**, SBBD14 (2021).

[17]M. Treu, R. Rupp, H. Kapels, and W. Bartsch, Mater. Sci. Forum **353–356**, 679 (2001).

[18]T. Hatakeyama and T. Shinohe, Mater. Sci. Forum **389–393**, 1169 (2002).

[19]J. Suda, K. Yamaji, Y. Hayashi, T. Kimoto, K. Shimoyama, H. Namita, and S. Nagao, Appl. Phys. Express **3**, 101003 (2010).

[20]M. Higashiwaki, K. Konishi, K. Sasaki, K. Goto, K. Nomura, Q. T. Thieu, R. Togashi, H. Murakami, Y. Kumagai, B. Monemar, A. Koukitu, A. Kuramata, and S. Yamakoshi, Appl. Phys. Lett. **108**, 133503 (2016).

[21]E. L. Murphy and R. H. Good, Phys. Rev. **102**, 1464 (1956).

[22]F. A. Padovani and R. Stratton, Solid State Electron. **9**, 695 (1966).

[23]R. Stratton, J. Phys. Chem. Solids **23**, 1177 (1962).

[24]T. Kimoto and J. A. Cooper, *Fundamentals of Silicon Carbide Technology: Growth, Characterization, Devices and Applications* (Wiley-IEEE Press, 2014).

[25]A. Itoh and H. Matsunami, Phys. Status Solidi A **162**, 389 (1997).

[26]W. A. Harrison, Phys. Rev. **123**, 85 (1961).

[27]W. Li, D. Jena, and H. G. Xing, J. Appl. Phys. **131**, 015702 (2022).

[28]S. M. Sze, Y. Li, and K. K. Ng, *Physics of Semiconductor Devices* (John Wiley & Sons, 2021).

[29]D. Volm, B. K. Meyer, D. M. Hofmann, W. M. Chen, N. T. Son, C. Persson, U. Lindefelt, O. Kordina, E. Sörman, A. O. Konstantinov, B. Monemar, and E. Janzén, Phys. Rev. B **53**, 15409 (1996).

[30]T. Kimoto and H. Watanabe, Appl. Phys. Express **13**, 120101 (2020).

[31]W. Li, D. Saraswat, Y. Long, K. Nomoto, D. Jena, and H. G. Xing, Appl. Phys. Lett. **116**, 192101 (2020).

[32]T. Doi, S. Shibayama, M. Sakashita, K. Kojima, M. Shimizu, and O. Nakatsuka, Appl. Phys. Express **15**, 015501 (2021).